

Influence of Mn diffusion on IrMn thickness threshold for the onset of exchange bias in IrMn/Co bilayers

G. Vinai, L. Frangou, C. Castán-Guerrero, V Bonanni, B Gobaut, S. Auffret,
I. L. Prejbeanu, B. Dieny, Vincent Baltz, P. Torelli

► **To cite this version:**

G. Vinai, L. Frangou, C. Castán-Guerrero, V Bonanni, B Gobaut, et al.. Influence of Mn diffusion on IrMn thickness threshold for the onset of exchange bias in IrMn/Co bilayers. *Journal of Physics: Conference Series*, IOP Publishing, 2017, 903, pp.012061. 10.1088/1742-6596/903/1/012061 . hal-01683639

HAL Id: hal-01683639

<https://hal.archives-ouvertes.fr/hal-01683639>

Submitted on 23 May 2019

HAL is a multi-disciplinary open access archive for the deposit and dissemination of scientific research documents, whether they are published or not. The documents may come from teaching and research institutions in France or abroad, or from public or private research centers.

L'archive ouverte pluridisciplinaire **HAL**, est destinée au dépôt et à la diffusion de documents scientifiques de niveau recherche, publiés ou non, émanant des établissements d'enseignement et de recherche français ou étrangers, des laboratoires publics ou privés.

Influence of Mn diffusion on IrMn thickness threshold for the onset of exchange bias in IrMn/Co bilayers

G Vinai¹, L Frangou², C Castan-Guerrero¹, V Bonanni^{1,3}, B Gobaut⁴, S Auffret², I L Prejbeanu², B Dieny², V Baltz², P Torelli¹

¹ Laboratorio TASC, IOM-CNR, S.S. 14 km 163.5, Basovizza, I-34149 Trieste, Italy

² SPINTEC, Univ. Grenoble Alpes / INAC-CEA / CNRS, F-38000 Grenoble, France

³ Department of Physics, University of Milan, Via Celoria 16, I-20133 Milan, Italy

⁴ Sincrotrone Trieste S.C.p.A., S.S.14 km 163.5, Area Science Park, 34149 Trieste, Italy

E-mail: vinai@iom.cnr.it

Abstract. In this work, we studied the influence of the buffer layer composition on the IrMn thickness threshold for the onset of exchange bias in IrMn/Co bilayers. By means of magnetometry, x-ray absorption and x-ray photoelectron spectroscopy, we investigated the magnetic and chemical properties of the stacks. We demonstrated a higher diffusion of Mn through the Co layer in the case of a Cu buffer layer. This is consistent with the observation of larger IrMn thickness threshold for the onset of exchange bias.

1. Introduction

Reducing the thickness of exchange biased stacks is of technological interest for applications in hard disk drives to allow larger data capacity. In this context, earlier publications demonstrated that an antiferromagnetic (AF) layer (e.g. IrMn) sandwiched between two ferromagnetic (F) layers, with out-of-plane (e.g. Pt/Co) and in-plane (e.g. Co) anisotropy respectively, exhibits lower AF thickness threshold (t_c) for the onset of exchange bias compared to simple IrMn/Co bilayers [1]. Here, further investigations were carried out in order to determine whether other mechanisms also contribute. We compared the chemical and magnetic properties of X/IrMn/Co exchange coupled thin films for different buffer layers (X). In particular, we focused our attention on Mn diffusion through the Co layer by x-ray absorption (XAS), x-ray magnetic circular dichroism (XMCD) and x-ray photoelectron spectroscopy (XPS) measurements.

2. Experimental procedure

A series of samples was deposited by dc-magnetron sputtering with an Ar pressure of $2.5 \cdot 10^{-3}$ mbar onto thermally oxidized silicon substrates, Si/SiO₂//. The stack was Ta₃/X/IrMn_{thickness}/Co₅/Pt₂ (nm). Ta layer was used to decouple the Si/SiO₂ substrate from the following layers. The buffer layers X were Cu₂, Pt₂, Pt_{7.2}, Ru_{7.2}, (Pt_{1.8}/Ru_{0.6})_{x3} and (Pt_{1.8}/Co_{0.6})_{x3} layers. IrMn layer was deposited from an Ir₂₀Mn₈₀ target (at. %). The top layer of Pt was used to prevent oxidation in air. The samples were annealed after deposition at 300°C in 10^{-6} mbar pressure and field cooled down to room temperature under an



applied in-plane magnetic field of 2 kOe. Hysteresis loops were measured on all samples at room temperature with a vibrating sample magnetometer.

XAS, XMCD and XPS measurements were performed at APE beamline at Elettra synchrotron [2]. Samples were measured at room temperature, with the beam impinging on the surface of the samples at 60° . Absorption spectra have been taken in circular polarization, clockwise (σ^+) and anti-clockwise (σ^-). The sum between the two spectra provides information on the chemical properties of the elements, whereas the difference represents the magnetic dichroic signal. Measurements were taken in total electron yield (TEY) mode, normalizing the sample current with the current coming on the mesh of the beamline. XAS and XMCD were performed at remanence after having saturated the samples along the direction of the setting field, by reversing the polarization of the circular light. In this way, no training effects on exchange bias had to be taken into account.

3. Results and discussion

Figure 1 shows the values of exchange bias (H_{ex}) and coercive field (H_C) for the whole series of samples. The variation of H_{ex} as a function of IrMn thickness follows the one expected for similar IrMn/Co stacks [3] for all buffer layers. For IrMn layers below t_C , no exchange bias is measured. For values between 2 and 4 nm, H_{ex} increases whereas H_C exhibits a maximum. The highest value of exchange bias appears between 4 and 5 nm, and then decreases for larger thicknesses. This trend is consistent with a granular model of exchange bias, which is commonly used for sputtered samples [4].

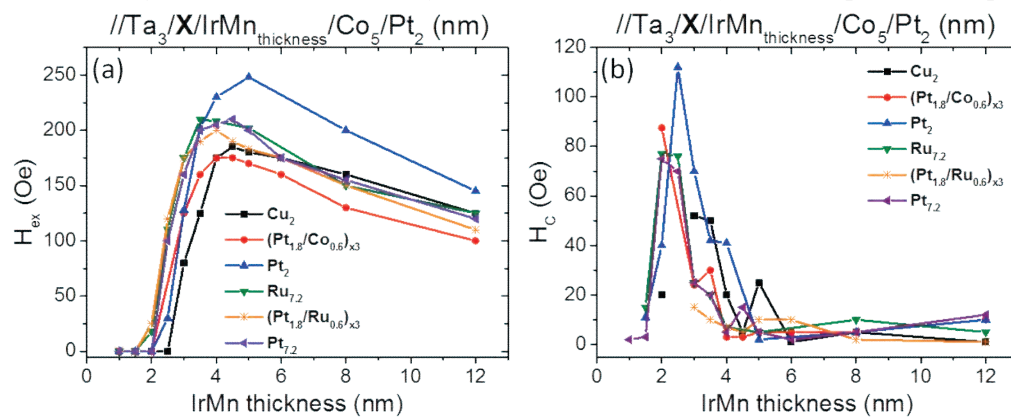


Figure 1. Exchange bias (a) and coercive (b) fields for the different stacks at room temperature.

From the full series of samples, those with an IrMn thickness of 3 nm (i.e. as the exchange bias increases with the IrMn thickness) have been selected. At this thickness, values of H_{ex} range from 80 Oe, for Cu_2 buffer layer, to twice this value, 175 Oe, for $\text{Ru}_{7.2}$ and $(\text{Pt}_{1.8}/\text{Ru}_{0.6})_{x3}$ buffer layers.

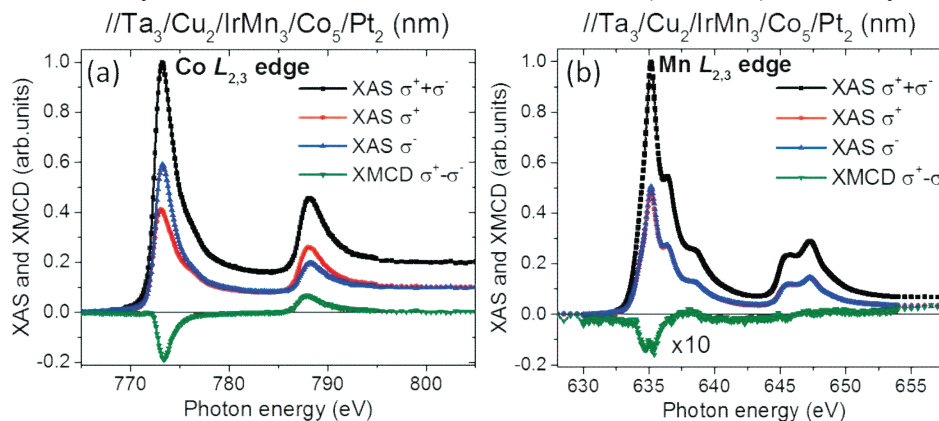


Figure 2. XAS and XMCD spectra at Co (a) and Mn (b) $L_{2,3}$ edges for $\text{Ta}_3/\text{Pt}_{7.2}/\text{IrMn}_3/\text{Co}_5/\text{Pt}_2$ sample.

Figure 2 shows the XAS and XMCD spectra at Co (a) and Mn (b) $L_{2,3}$ edges for the $\text{Ta}_3/\text{Pt}_{7.2}/\text{IrMn}_3/\text{Co}_5/\text{Pt}_2$ sample. XAS and XMCD curves have been normalized to the sum of the two circularly polarized spectra. Co absorption spectrum is characteristic of metallic Co and shows no traces of oxidation [5], which indicates the successful protection by the 2 nm Pt capping. Different buffer layers yield no changes in Co spectra shape. Mn absorption spectrum (figure 2b) also reveals no signs of oxidation, as a fully metallic Mn spectrum [6]. Considering that the penetration depth of TEY measurements is of only a few nm, the weak XAS signal measured at Mn edge, because of the covering by the 2 nm of Pt and 5 nm of Co layers, comes from the Mn atoms at the IrMn/Co interface.

From magnetic point of view, we can notice that both Co and Mn XMCD spectra have the same sign, which corresponds to a ferromagnetic coupling across the IrMn/Co interface, as reported in the literature [7]. This has been confirmed for all buffer layers. Co dichroic signal, by taking into account the angle of 60° of the sample with respect to the beam and a polarization level of 75%, is around 29%. By applying the sum rules [8], we evaluate a total magnetic moment of Co of $2.3 \mu_B$, which corresponds to typical bulk value. Similar values were obtained for all samples. Regarding Mn, the XMCD spectrum has been magnified by a factor 5 in order to be clearly visible. Its dichroic intensity of around 4% with comparison with the one of Co confirms that only a slight percentage of spins participate to the exchange. In this case, signal intensity and signal-over-noise ratio give error bars too large to apply sum rules. XAS and XMCD measurements at Mn edge were also performed with the samples oriented normal to the beam incidence. In this configuration, no magnetic dichroic signal was measured. This means that the uncompensated Mn spins are aligned in-plane with the Co spins, with no out-of-plane canting.

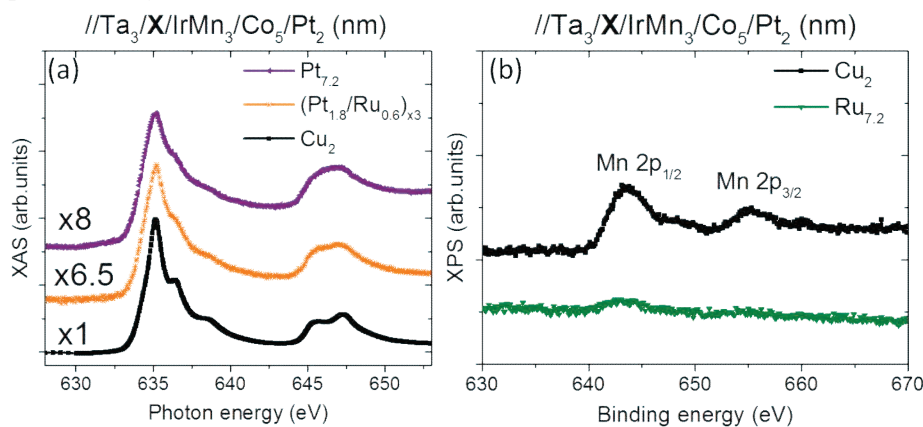


Figure 3. (a) Comparison between XAS spectra at Mn edges for different buffer layers. Curves have been normalized to Cu_2 buffered sample; (b) Mn $2p$ XPS spectra for Cu_2 and $\text{Ru}_{7.2}$ buffer layers.

Concerning the absorption spectra at Mn edge, $\text{Ta}_3/\text{Cu}_2/\text{IrMn}_3/\text{Co}_5/\text{Pt}_2$ sample differed from all other buffer layers. In figure 3(a), we show the XAS curves for three different buffer layers. Curves have been normalized to the signal intensity of Cu_2 buffered sample. In order to do so, the spectra of $\text{Pt}_{7.2}$ and $(\text{Pt}_{1.8}/\text{Ru}_{0.6})_{\times 3}$ buffered samples had to be multiplied by a factor 8 and 6.5 respectively. It has to be stressed that all measurements were performed in identical beamline conditions, thus the comparison between background-to-peak intensity at L_3 edges between different samples gives information on the location of Mn atoms through the thickness of the sample, since the signal intensity exponentially decreases while penetrating into the sample. Moreover, the shape of Mn absorption spectra for Cu_2 buffered sample strongly differs from other samples. It presents features which can be attributed to a partial oxidation of Mn, which appears in the $3d^5$ configuration of Mn^{2+} in octahedral symmetry [9]. One possible reason for such differences among the Mn spectra is the incomplete covering of the Pt capping layer for the Cu_2 buffered sample. In order to verify this, nominally identical samples deposited in different periods with Cu_2 buffer layer were compared, giving identical XAS. We thus consider that such feature is intrinsic to the sample.

In order to investigate the reason of such differences, XPS measurements were performed on all samples of the series setting the beamline energy at $h\nu = 1000$ eV. This kind of measurement is more surface sensitive than XAS, with a penetration depth of roughly one nm. As it can be seen from figure 3(b), in case of Cu₂ buffer layer Mn 2*p* levels were measured, whereas in the case of Ru_{7,2} no sign of Mn was observed. Curves have been normalized at Pt 4*f* levels.

By comparing XAS raw measurements of figure 3(a) and XPS Mn 2*p* spectra of figure 3(b), we can state that in case of Cu₂ buffer layer Mn diffused throughout the Co layer up to the surface, resulting in a higher level of oxidation compared to other samples. The interdiffusion of Mn most probably took place during the annealing process at 300°C, necessary to set the exchange bias coupling. Mn atoms which diffused up to the surface experience an oxidation process, as observed by XAS measurement. In this case, most of the absorption signal comes from the Mn atoms close to the surface, hiding the signal of metallic Mn atoms present at the IrMn/Co interface. Interdiffusion is a critical aspect from technological point of view, because of the annealing steps necessary in the devices processing. It has been shown that interdiffusion takes place preferentially along grain boundaries [10], with levels of diffusions which vary with annealing temperature.

From the XAS and XPS measurements performed, we observe that not only the layers over IrMn play a role on Mn diffusion to the surface, but also buffer layers do. Whereas Pt and Ru layers help limiting the Mn diffusion, Cu does not. Indeed, Cu tends to form large grains separated by pronounced grain boundaries favoring atomic mobility. This has consequences on exchange bias field value. The Cu₂ buffer yields the largest t_C characterizing the onset of H_{ex} , likely because of a strong reduction in the AF intergrain exchange coupling across the grain boundaries. For all other samples, wherein IrMn is unoxidized and interdiffusion is very limited, H_{ex} is maximized.

4. Acknowledgments

This work has been partly performed in the framework of the nanoscience foundry and fine analysis (NFFA-MIUR Italy Progetti Internazionali) project.

References

- [1] Vinai G, Moritz J, Bandiera S, Prejbeanu I L and Dieny B 2013 *J. Phys. D.: Appl. Phys.* **46** 322001
- [2] Panaccione G, Vobornik I, Fujii J, Krizmancic D, Annese E, Giovanelli L, Maccherozzi F, Salvador F, De Luisa A, Benedetti D, Gruden A, Bertoch P, Polack F, Cocco D, Sostero G, Diviaco B, Hochstrasser M, Maier U, Pescia D, Back C H, Greber T, Osterwalder J, Galaktionov M, Sancrotti M and Rossi G 2009 *Rev. Sci. Instrum.* **80** 043105
- [3] Ali M, Marrows C, Al-Jawad M, Hickey B, Misra A, Nowak U and Usadel K 2003 *Phys. Rev. B* **68** 214420
- [4] O'Grady K, Fernandez-Outon L E and Vallejo-Fernandez G 2009 *J. Magn. Magn. Mater.* **322** 883
- [5] Regan T, Ohldag H, Stamm C, Nolting F, Lüning J, Stöhr J and White R 2001 *Phys. Rev. B* **64** 214422
- [6] Torelli P, Sirotti F and Ballone P 2003 *Phys. Rev. B* **68** 205413
- [7] Takahashi H, Kota Y, Tsunoda M, Nakamura T, Kodama K, Sakuma A and Takahashi M 2011 *J. Appl. Phys.* **110** 123920
- [8] Chen C T, Idzerda Y U, Lin H -J, Smith N V, Meigs G, Chaban E, Ho G H, Pellegrin E and Sette F 1995 *Phys. Rev. Lett.* **75** 152
- [9] Eimüller T, Kato T, Mizuno T, Tsunashima S, Quitmann C, Ramsvik T, Iwata S and Schütz G 2004 *Appl. Phys. Lett.* **85** 2310
- [10] Letellier F, Lechevallier L, Lardé R, Le Breton J M, Akmalidinov K, Auffret S, Dieny B and Baltz V 2014 *J. Appl. Phys.* **116** 203906